Brownian Ratchet in a Thermal Bath Driven by Coulomb Friction

Andrea Gnoli

Istituto dei Sistemi Complessi-CNR, via del Fosso del Cavaliere 100, 00133 Rome, Italy and Istituto dei Sistemi Complessi-CNR and Dipartimento di Fisica, Università "Sapienza", Piazzale Aldo Moro 2, 00185 Rome, Italy

Alberto Petri, Fergal Dalton, and Giorgio Pontuale

Istituto dei Sistemi Complessi-CNR, via del Fosso del Cavaliere 100, 00133 Rome, Italy

Giacomo Gradenigo, Alessandro Sarracino, and Andrea Puglisi

Istituto dei Sistemi Complessi-CNR and Dipartimento di Fisica, Università "Sapienza", Piazzale Aldo Moro 2, 00185 Rome, Italy

(Received 15 November 2012; published 19 March 2013)

The rectification of unbiased fluctuations, also known as the ratchet effect, is normally obtained under statistical nonequilibrium conditions. Here we propose a new ratchet mechanism where a thermal bath solicits the random rotation of an asymmetric wheel, which is also subject to Coulomb friction due to solid-on-solid contacts. Numerical simulations and analytical calculations demonstrate a net drift induced by friction. If the thermal bath is replaced by a granular gas, the well-known granular ratchet effect also intervenes, becoming dominant at high collision rates. For our chosen wheel shape the granular effect acts in the opposite direction with respect to the friction-induced torque, resulting in the inversion of the ratchet direction as the collision rate increases. We have realized a new granular ratchet experiment where both these ratchet effects are observed, as well as the predicted inversion at their crossover. Our discovery paves the way to the realization of micro and submicrometer Brownian motors in an equilibrium fluid, based purely upon nanofriction.

DOI: 10.1103/PhysRevLett.110.120601 PACS numbers: 05.60.−k, 05.20.Dd, 05.40.−a, 81.05.Rm

From microscopic organisms to muscle fibers, from electric motors to power stations, the biosphere, our society, and our lives critically depend on the conversion of energy to mechanical work. Thermodynamics provides precise and well-established rules for energy conversion in macroscopic systems but these rules become blurred at small scales when thermal fluctuations play a decisive role [1]. Extracting work under such conditions requires subtle strategies radically different from those effective in the macroscopic world [2–7]. Within this framework, the theory of Brownian motors deals with the rectification of thermal fluctuations, a goal which can only be achieved in the presence of dissipation [8–13]. An interesting class of systems, where both dissipation and fluctuations are relevant, is represented by granular media [14,15]. Indeed, interactions in a granular system are inherently dissipative, and because of its small number of constituents when compared with molecular gases or liquids, a granular fluid presents large fluctuations. The additional break of spatial symmetry is sufficient for a motor effect to be generated as demonstrated in a series of experiments [16–19] and theoretical works [20–25].

In previous work the main source of dissipation was provided by the inelasticity of collisions, a property normally not present at micro or nanometric scales. The remarkable result of our study is a new minimal model for a motor where energy is extracted from an equilibrium bath and dissipated only through Coulomb friction [26]. Friction is therefore demonstrated to be an unexpectedly efficient source of dissipation that is able to rectify unbiased fluctuations also in the case of *fully elastic* collisions. Such a model can therefore be exploited in micro and nano apparatuses where friction is still present [27].

Our model, described pictorially in Fig. 1(a), consists of a wheel of mass M and moment of inertia I, rotating with angular velocity ω around a fixed axis (say $\hat{z}$). The wheel is immersed in an equilibrium fluid and collides with the molecules of mass m, and is subject to a viscous drag $-\Gamma_{visc}\omega$ and, most importantly, to a Coulomb friction torque $-F_{friction}\sigma(\omega)$ [where $\sigma(x)$ is the sign function], due to solid-on-solid contacts within its support, e.g., a

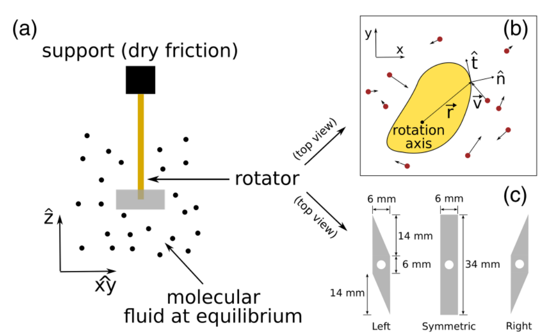

FIG. 1 (color online). (a) Sketch of the model, front view. (b) Top view, with explanation of quantities used in the text for a generic-shaped rotator. (c) Top view, with specific shapes used in the simulations and in the experiment.

spherical bearing. The equation of motion for the angular velocity $\omega(t)$ of the wheel, therefore, reads

$$\dot{\omega}(t) = -\gamma_a \omega(t) - \sigma[\omega(t)]\Delta + \eta_{\rm coll}(t), \qquad (1)$$

where $\gamma_a = \Gamma_{\rm visc}/I$, $\Delta = F_{\rm friction}/I$ and $\eta_{\rm coll}(t)$ is the random force due to collisions with the molecules of the bath. The wheel is a cylinder parallel to the rotation axis $\hat{z}$. Its base in the plane $\hat{x}\hat{y}$ [shown in Fig. 1(b) for a generic shape] can be symmetric or asymmetric for inversion of one of the two axis ($\hat{x}$ or $\hat{y}$). The two specific shapes taken in consideration here, one symmetric and other asymmetric, are drawn in Fig. 1(c). The velocities of the molecules are distributed according to the Maxwell-Boltzmann distribution, with the only parameter being the "thermal" velocity $v_0 = \sqrt{\langle v^2 \rangle}$, where v is a component of the velocity vector on the $\hat{x}\hat{y}$ plane. The molecular bath is also characterized by its number density n. The main parameter for the collision between the wheel and the molecules is the total cross section Σ. The collision rule, given in detail in the Supplemental Material [28], conserves total angular momentum and may dissipate part of the total kinetic energy, according to the value of the restitution coefficient $\alpha \in [0, 1]$. We will show that our model exhibits the ratchet effect even in the case of fully elastic collisions ($\alpha = 1$), and even if the viscous force is removed ($\gamma_a = 0$). The choice of a more general (possibly inelastic) collision rule and the presence of a weak viscous damping is necessary to account for the results of the granular experiment described below. For consistency with the experiment, the viscous force (if present) is assumed to be small enough that $\gamma_a|\omega| \ll \Delta$ for most of the values of ω.

When the range of interactions with the molecules is short enough (as in the hard-core case), only two time scales are relevant in the system: (i) the mean stopping time due to environmental dissipation, dominated by Coulomb friction, $\tau_\Delta = \frac{\langle|\omega|\rangle_{\rm pc}}{\Delta} \sim \frac{\epsilon v_0}{R_I \Delta}$, where $\langle \cdot \rangle_{\rm pc}$ denotes a postcollisional average, $R_I = \sqrt{I/M}$ is the radius of inertia and $\epsilon = \sqrt{m/M}$; (ii) the mean free time between two collisions $\tau_c \sim \frac{1}{n \Sigma v_0}$. We therefore use as the main control parameter

$$\beta^{-1} = \frac{\epsilon n \Sigma v_0^2}{\sqrt{2}\pi R_I \Delta} \approx \frac{\tau_\Delta}{\tau_c}, \qquad (2)$$

which is an estimate of the ratio of those two time scales, as verified by simulations [28]. As already noticed [23,24], when $\beta^{-1} \gg 1$ ($\tau_c \ll \tau_\Delta$) the dynamics of the rotator is dominated by collisions and friction is negligible (frequent collisions limit, denoted in the following by FCL); in the opposite limit $\beta^{-1} \ll 1$ ($\tau_c \gg \tau_\Delta$, rare collisions limit, RCL) the rotator remains most of the time at rest and is rarely perturbed by collisions acting as independent random excitations.

The complex behavior of the model is simplified in the diluted limit, when molecular chaos can be assumed. With such an assumption, the probability density function $p(\omega, t)$ for the angular velocity is fully described by the following linear Boltzmann equation [23,25,29]

$$\partial_t p(\omega, t) = \partial_\omega[(\Delta\sigma(\omega) + \gamma_a \omega) p(\omega, t)] + J[p, \phi], \qquad (3a)$$

$$J[p, \phi] = \int d\omega' W(\omega|\omega') p(\omega', t) - p(\omega, t) f_c(\omega), \qquad (3b)$$

where we introduce the rate $W(\omega'|\omega)$ for the transition $\omega \to \omega'$ and the velocity-dependent collision frequency $f_c(\omega) = \int d\omega' W(\omega'|\omega)$. The rate $W(\omega'|\omega)$, given explicitly for hard-core interactions in Ref. [28] depends on the velocity distribution of the gas particles, on the restitution coefficient α, on the rotator cross section, and on the density of the gas.

A first insight into Eq. (3) is obtained by direct Monte Carlo simulation [28,30], whose results are summarized in Fig. 2, always keeping $\gamma_a = 0$. The figure shows the average velocity of the ratchet rescaled by the ideal "thermal" velocity, i.e., $\langle \Omega \rangle = \frac{R_I}{\epsilon v_0} \langle \omega \rangle$, for several values of α and different shapes. Our main, unprecedented, result is the existence of an average drift, i.e., a motor effect, in the case of elastic collisions, provided that the shape is asymmetric (curve with diamond symbols). This effect is independent of the presence of the viscous damping, which very weakly affects the results of the simulation. In the elastic case, the average drift disappears for large β^{-1}, precisely for $\tau_\Delta \gtrsim \tau_c \epsilon^{-2}$, where $\tau_c \epsilon^{-2}$ is the characteristic time for thermalization of the probe due to collisions with the bath [25,31]. Remarkably, the ratchet effect starting from the RCL increases, in absolute value, when β^{-1} increases, so that it must go through a maximum. We

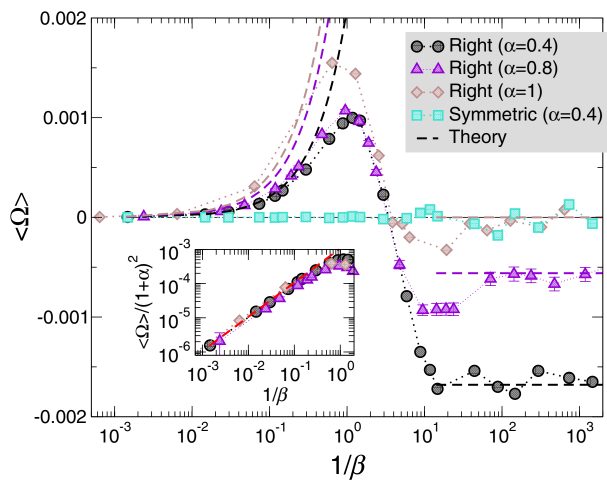

FIG. 2 (color online). Simulations under the assumption of molecular chaos. The rescaled average angular velocity $\langle \Omega \rangle$ is shown as a function of β^{-1}. Theoretical expectations in the FCL and RCL are marked by dashed lines. The lower inset zooms in the RCL region. Simulations are performed using shapes and dimensions of Fig. 1(c), $\Delta = 10$, $\gamma_a = 0$, $R_I/\epsilon = 10^3$, and $v_0 = 100$ in arbitrary units (varying $n\Sigma$ to obtain a variation of β^{-1}).

interpret such a maximum as a kind of *stochastic resonance*: the rotator switches from the "drift" state to the "rest" state on the time scale τ_Δ and switches back to the drift state on the time scale τ_c. When the two scales synchronize with each other, the total time spent in the drift state is maximized, as well as its average velocity.

As demonstrated in previous studies [20,21], in the inelastic case ($\alpha < 1$) a ratchet effect survives also in the FCL: interestingly, it takes different signs with respect to the RCL. Therefore, the crossover between these two limits requires the presence of an inversion point.

It is possible to have an analytical account of the two opposite RCL and FCL limits [23,25]. When the mass of the rotator is large, $\epsilon \ll 1$ the FCL is perturbatively reduced to a Brownian approximation and the average drift has already been computed [25], giving

$$\langle\Omega\rangle = \epsilon\sqrt{\frac{\pi}{2}}\frac{1-\alpha}{4}\mathcal{A}_{\rm FCL}, \quad (4a)$$

$$\mathcal{A}_{\rm FCL} = -\frac{\langle g^3\rangle_{\rm surf}}{\langle g^2\rangle_{\rm surf}}, \quad (4b)$$

where the asymmetry of the rotator is represented by $\mathcal{A}_{\rm FCL}$ which is 0 for a symmetric rotator; above we have used the shorthand notation for the uniform average along the perimeter (denoted as "surface") of the base of the wheel $\langle\rangle_{\rm surf} = \int_{\rm surf}\frac{ds}{S}$ (S being the total perimeter [28]), while $g = \frac{\mathbf{r}\cdot\hat{t}}{R_I}$; see Fig. 1(b) for an explanation of symbols. This formula predicts zero net drift either with elastic collisions ($\alpha = 1$) or with a symmetric rotator ($\mathcal{A}_{\rm FCL} = 0$), as expected from symmetry arguments. Most importantly, it predicts a constant value, as verified in the numerical simulations. This implies $|\langle\omega\rangle| \sim v_0$ for the *dimensional* angular velocity.

The study of the RCL leads to remarkably different predictions. In such a limit, the dynamics after each collision event produces an increment of the angular position of the rotator $\Delta\theta$ which depends on the velocity $\mathbf{v}$ of the gas particle, precisely on its projection $v = \mathbf{v}\cdot\hat{n}$, and on the point of impact represented by its curvilinear abscissa s. The formula is $\Delta\theta(v,s) = \sigma(\omega_0)\frac{\omega_0^2}{2\Delta}$ with $\omega_0 = -(1+\alpha)\frac{v}{R_I}\frac{\epsilon^2 g}{1+\epsilon^2 g^2}$. Following the calculations detailed in Ref. [28], one obtains the formula for the rescaled average velocity of the ratchet

$$\langle\Omega\rangle = \sqrt{\pi}(1+\alpha)^2\beta^{-1}\epsilon^2\mathcal{A}_{\rm RCL}, \quad (5a)$$

$$\mathcal{A}_{\rm RCL} = \left\langle\frac{\sigma(g)g^2}{(1+\epsilon^2 g^2)^2}\right\rangle_{\rm surf}, \quad (5b)$$

where $\mathcal{A}_{\rm RCL} = 0$ for symmetric shapes of the rotator. Equation (5) shows that a nonzero drift is achieved *for any value of the restitution coefficient*: even in the (ideal) elastic case, Coulomb friction alone produces the desired ratchet effect provided that the shape of the rotator is not symmetric, i.e., that $\mathcal{A}_{\rm RCL} \neq 0$. Note that the limit of vanishing dry friction ($\Delta \to 0$) is singular in formula (5a), since in the absence of dissipation between collisions the stopping time becomes infinite, $\tau_\Delta \to \infty$, and the assumption of "rare collisions" breaks down. Equally interesting, the shape factor $\mathcal{A}_{\rm RCL}$, determining the intensity and drift direction in the RCL, can take *opposite sign* with respect to the shape factor $\mathcal{A}_{\rm FCL}$ in the FCL formula. This is precisely the case for our chosen shape; see Fig. 1(c). Moreover, the magnitude of the drift is predicted to increase with β^{-1} as seen in the numerical simulations for small β^{-1}. This corresponds to $|\langle\omega\rangle| \sim v_0^3$. Both the predictions for the RCL and for the FCL are superimposed on the results (elastic and inelastic) of the numerical simulations in Fig. 2, demonstrating excellent agreement in their respective limits. We remark that if friction is removed ($\Delta = 0$) the only ratchet effect is the one predicted in Eq. (4); i.e., no inversion is observed.

In order to obtain the first experimental evidence of this newly discovered ratchet effect, we have built a macroscopic realization of our model, i.e., a setup where the thermal bath is replaced by a fluidized granular gas. In such a setup the collisions are unavoidably inelastic: nonetheless, by tuning the collision frequency, it is possible to disentangle the two ratchet mechanisms which act in opposite directions, and so demonstrate the newly discovered effect induced by Coulomb friction. Our setup consists of a rotator vertically suspended in a granular medium [see Fig. 3(a)] maintained by an electrodynamic shaker in a (roughly homogeneous) stationary gaseous regime [15,32]. The statistics of the velocities of the grains, on the rotation plane, has been verified to be indistinguishable from a Maxwell-Boltzmann distribution [28]. The shaker performs a vertical sinusoidal oscillation at a frequency of 53 Hz, while the amplitude is varied to explore different regimes of the system. We stress that the rotator is not in direct contact with the shaker, it only collides with the flying grains. Its motion is recorded by an angular encoder which also supports it through two precision spherical bearings. Two rotators have been realized to reproduce

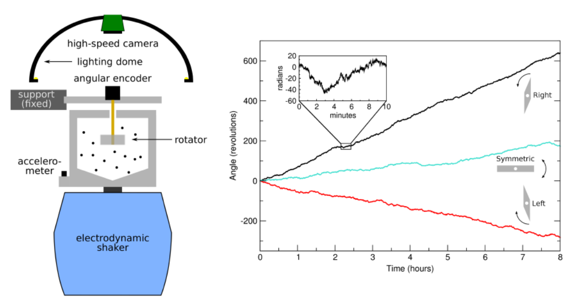

FIG. 3 (color online). Real experiment. (a) Experimental setup. (b) The angular position of the rotator as a function of time, highlighting the ratchet effect for the asymmetric rotator. The inset shows an enlargement (10 min) extracted from a asymmetric (right) experiment. For these experiments the value of maximum acceleration, normalized by gravity, is 13.

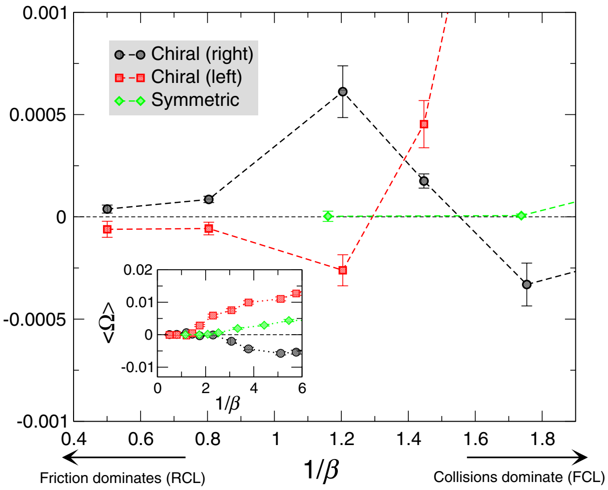

FIG. 4 (color online). Real experiment. Plot of the rescaled angular velocity of the rotator, $\langle\Omega\rangle = \frac{R_I}{\epsilon v_0}\langle\omega\rangle$, averaged on an 8-h run, as a function of β^{-1} which estimates the ratio of time scales $\frac{\tau_\Delta}{\tau_c}$. The main plot shows the region where a maximum and a current inversion are observed for the asymmetric rotator. The inset sums up all the results, highlighting the behavior for large β^{-1}. Experiments are performed with maximum shaker acceleration varying in the range from 5 to 20 in gravity units.

the two different shapes of Fig. 1(c). The asymmetry of the latter can be inverted (from left- to right-hand, and vice versa) simply by turning the rotator upside down. The amplitude of the shaker oscillation is varied to span a range of maximum acceleration (in units of gravity acceleration) between 5 to 20, resulting in a granular thermal velocity v_0 ranging between ~100 mm/s and ~600 mm/s. Details of the experimental setup and measurement of the parameters are in Ref. [28].

In Fig. 3(b), we provide some runs demonstrating the ratchet effect for the asymmetric rotator. A net drift is evident when a chiral rotator is used. Turning the rotator upside down results in a reversed direction of rotation. The symmetric rotator makes a diffusive motion with only a small drift revealing the presence of some bias due to imperfections in the rotational symmetry of the setup. Such a bias affects also the curves pertaining to the asymmetric rotator and it does not appear to depend on the rotator's direction of asymmetry, or absence thereof. The typical instantaneous velocity of rotators goes from $\sim 10^{-1}$ to ~1 rad/s, much larger than the typical ratchet drift, which goes from $\sim 10^{-4}$ to 10^{-2} rad/s. Such a low signal-to-noise ratio makes it impossible to determine the true behavior of the rotator if one monitors its position only for short times (e.g., less than a few hours), as evidenced in the inset of Fig. 3(b).

In Fig. 4, we show the average adimensional angular velocity $\langle\Omega\rangle = \frac{R_I}{\epsilon v_0}\langle\omega\rangle$ for a set of experiments with asymmetric and symmetric rotators. The behavior with β^{-1} strongly resembles that observed in our numerical simulations (Fig. 2). At $\beta^{-1} < 1$, we measure $|\langle\Omega\rangle|$ increasing with β^{-1}, followed by a maximum in the proximity of $\beta^{-1} \sim 1$ and then by an inversion of direction of motion. At large β^{-1}, $|\langle\Omega\rangle|$ increases and finally reaches a plateau (see the inset of Fig. 4). Even with some quantitative discrepancies, we can claim that our experiment reproduces very well the qualitative phenomenology of the model, including the resonant maximum and the inversion point, which are both evidence of the presence of the friction-induced ratchet mechanism. We believe that the quantitative differences (the real ratchet is faster roughly by a factor 2 in the RCL and a factor 5 in the FCL) can be imputed to the many assumptions present in the model, the most important being molecular chaos and spatial homogeneity, hardly controlled in the experiment: indeed nonequilibrium correlations may well become important at high collision frequencies [33].

To conclude, our main discovery is the existence of a minimal ratchet model made of two simple ingredients: a wheel subject to Coulomb friction and a bath at thermodynamic equilibrium. Such a model appears even simpler than the classical Feynman-Smoluchowski model [9]. The observation in the laboratory of a maximum and an inversion of the ratchet velocity (Fig. 4), due to the crossover from the inelasticity-dominated (FCL) to the friction-dominated (RCL) regime, is a strong experimental demonstration of the efficiency of this effect. We wish to remark that, in all previous experimental and theoretical work on friction-driven ratchets [34–37], the energy injection was provided by mechanisms different from an equilibrium bath: our proposal is the first which can be realized at the micro- and nanoscale in an equilibrium fluid, that is, without the application of any external field.

We would like to thank A. Vulpiani for useful comments and MD. Deen for technical support. The authors acknowledge the support of the Italian MIUR under the Grants FIRB-IDEAS No. RBID08Z9JE, FIRBs No. RBFR081IUK and No. RBFR08M3P4, and PRIN No. 2009PYYZM5.

[1] T. L. Hill, *Thermodynamics of Small Systems* (Dover, New York, 1964).
[2] M. Schliwa and G. Woehlke, Nature (London) **422**, 759 (2003).
[3] S. Rice *et al.*, Nature (London) **402**, 778 (1998).
[4] I. Rayment, W. R. Rypniewski, K. Schmidt-Base, R. Smith, D. Tomchick, M. M. Benning, D. A. Winkelmann, G. Wesenberg, and H. M. Holden, Science **261**, 50 (1993).
[5] R. Di Leonardo, L. Angelani, D. Dell'Arciprete, G. Ruocco, V. Iebba, S. Schippa, M. P. Conte, F. Mecarini, F. De Angelis, and E. Di Fabrizio, Proc. Natl. Acad. Sci. U.S.A. **107**, 9541 (2010).
[6] A. Sokolov, M. M. Apodaca, B. A. Grzybowski, and I. S. Aranson, Proc. Natl. Acad. Sci. U.S.A. **107**, 969 (2010).

[7] G. Gradenigo, A. Sarracino, D. Villamaina, T. S. Grigera, and A. Puglisi, J. Stat. Mech. (2010) L12002.
[8] M. v. Smoluchowski, Phys. Z. **13**, 1069 (1912).
[9] R. P. Feynman, R. B. Leighton, and M. Sands M, *The Feynman Lectures on Physics* (Addison-Wesley, Reading, MA, 1963), Vol. I, Chap. 46.
[10] M. O. Magnasco, Phys. Rev. Lett. **71**, 1477 (1993).
[11] R. D. Astumian, Science **276**, 917 (1997).
[12] P. Reimann, Phys. Rep. **361**, 57 (2002).
[13] P. Hänggi and F. Marchesoni, Rev. Mod. Phys. **81**, 387 (2009).
[14] H. M. Jaeger, S. R. Nagel, and R. P. Behringer, Rev. Mod. Phys. **68**, 1259 (1996).
[15] G. D'Anna, P. Mayor, A. Barrat, V. Loreto, and F. Nori, Nature (London) **424**, 909 (2003).
[16] Z. Farkas, P. Tegzes, A. Vukics, and T. Vicsek, Phys. Rev. E **60**, 7022 (1999).
[17] P. Eshuis, K. van der Weele, D. Lohse, and D. van der Meer, Phys. Rev. Lett. **104**, 248001 (2010).
[18] R. Balzan, F. Dalton, V. Loreto, A. Petri, and G. Pontuale, Phys. Rev. E **83**, 031310 (2011).
[19] M. Heckel, P. Müller, T. Pöschel, and J. A. C. Gallas, Phys. Rev. E **86**, 061310 (2012).
[20] G. Costantini, U. Marini Bettolo Marconi, and A. Puglisi, Phys. Rev. E **75**, 061124 (2007).
[21] B. Cleuren and C. Van den Broeck, Europhys. Lett. **77**, 50 003 (2007).
[22] G. Costantini, U. Marini Bettolo Marconi, and A. Puglisi, Europhys. Lett. **82**, 50 008 (2008).
[23] J. Talbot, R. D. Wildman, and P. Viot, Phys. Rev. Lett. **107**, 138001 (2011).
[24] J. Talbot, A. Burdeau, and P. Viot, J. Stat. Mech. (2011) P03009.
[25] B. Cleuren and R. Eichhorn, J. Stat. Mech. (2008) P10011.
[26] B. N. J. Persson, *Sliding Friction* (Springer, Berlin, 1998).
[27] R. Guerra, U. Tartaglino, A. Vanossi, and E. Tosatti, Nat. Mater. **9**, 634 (2010).
[28] See Supplemental Material at http://link.aps.org/supplemental/10.1103/PhysRevLett.110.120601 for details on experimental setup, theory, and simulations.
[29] N. G. van Kampen, Can. J. Phys. **39**, 551 (1961).
[30] G. A. Bird, *Molecular Gas Dynamics and the Direct Simulation of Gas Flows* (Clarendon, Oxford, 1994).
[31] A. Sarracino, D. Villamaina, G. Costantini, and A. Puglisi, J. Stat. Mech. (2010) P04013.
[32] A. Naert, Europhys. Lett. **97**, 20 010 (2012).
[33] G. Gradenigo, A. Sarracino, D. Villamaina, and A. Puglisi, Europhys. Lett. **96**, 14 004 (2011); A. Sarracino, D. Villamaina, G. Gradenigo, and A. Puglisi, Europhys. Lett. **92**, 34 001 (2010).
[34] M. Eglin, M. A. Eriksson, and R. W. Carpick, Appl. Phys. Lett. **88**, 091913 (2006).
[35] A. Buguin, F. Brochard, and P.-G. de Gennes, Eur. Phys. J. E **19**, 31 (2006).
[36] D. Fleishman, J. Klafter, M. Porto, and M. Urbakh, Nano Lett. **7**, 837 (2007).
[37] A. Baule and P. Sollich, Europhys. Lett. **97**, 20 001 (2012).